

Extent of sensitivity of single photon production to parton distribution functions

SOMNATH DE

Variable Energy Cyclotron Centre, 1/AF Bidhan Nagar, Kolkata 700 064, India
E-mail: somvecc@gmail.com

MS received 19 September 2013; accepted 13 December 2013

DOI: 10.1007/s12043-014-0765-y; ePublication: 29 May 2014

Abstract. We have studied the production of single isolated prompt photons in high-energy proton–proton collisions at the RHIC ($\sqrt{s} = 200$ GeV) and the LHC ($\sqrt{s} = 7$ TeV) energies within the framework of perturbative QCD upto next-to-leading order of strong coupling (α_s). We have used five different parametrizations of parton distribution function (PDF) starting from the old CTEQ4M to the new CT10 distributions and compared our results with the recent single-prompt photon data from the PHENIX and the CMS Collaborations. The prompt photon cross-section is found to be described equally well by all the PDFs within the experimental errors at the RHIC and the LHC energies. The deviation in the single-prompt photon yield for different PDF sets is within $\pm 20\%$ when compared to CTEQ4M, indicating the upper bound of uncertainty in determining the gluon density. The diphoton measurement could be a potential candidate to constrain the gluon distribution inside the proton.

Keywords. Prompt photon; parton distribution function; perturbative quantum chromodynamics.

PACS Nos 13.75.Cs; 12.38.Bx; 25.75.Dw; 13.85.Qk

1. Introduction

The production of single-prompt photons of large transverse momenta in high-energy hadronic collisions constitutes unique signal of the interactions between quarks and gluons at short distances [1]. The single-prompt photon yield is expected to be sensitive to parton distribution function (PDF) in general and to gluon distribution in particular of the colliding hadron [2–9]. It is also considered an essential ingredient to quantify the nuclear modification of direct photon production in the relativistic nucleus–nucleus collisions [10]. The word ‘prompt’ is used to identify the class of photons that do not come from the decay of large-momenta hadrons (e.g., π^0 , η , etc.). The basic mechanisms of prompt photon production at the leading-order (LO) of strong coupling α_s are: (i) quark–gluon Compton scattering ($qg \rightarrow q\gamma$), (ii) quark–antiquark annihilation ($q\bar{q} \rightarrow g\gamma$) and (iii) bremsstrahlung radiation from the final-state parton ($q(g) \rightarrow q(g) + \gamma$) [1].

Because of the point-like coupling, the photons produced through the processes (i) and (ii) are called ‘direct’ photons. The direct photons are often calculated using perturbative quantum chromodynamics (pQCD), which successfully explains the production of particles with energy $E \gg \Lambda_{\text{QCD}}$ (where $\Lambda_{\text{QCD}} \sim 200$ MeV). The photons originated from the process (iii) are called ‘fragmentation’ photons. The evaluation of this contribution requires non-perturbative parton to photon fragmentation function as an input along with pQCD. However, at this point, we must state that the distinction is renormalization scheme-dependent and has no physical implication beyond LO. A complete next-to-leading order (NLO) theory is needed to explain the single- and double-prompt photon data in hadronic collisions [11].

The momentum fraction probed by the prompt photon of transverse momentum p_{T}^{γ} for proton–proton ($p + p$) collisions at midrapidity ($y = 0$) is given by $x \approx 2p_{\text{T}}^{\gamma}/\sqrt{s}$ where \sqrt{s} is the centre of mass energy. The photon production is more sensitive to the gluon distribution at low p_{T}^{γ} (i.e., small x) and to the valance quark distribution towards higher p_{T}^{γ} (i.e., large x) for a fixed \sqrt{s} . Thus, one can hope to determine the gluon distribution $g(x, Q^2)$ unambiguously from the very accurate prompt photon data.

The present work is aimed to verify the above assumptions. For this purpose, we have considered the isolated prompt photon production in $p + p$ collisions at the Relativistic Heavy Ion Collider (RHIC) ($\sqrt{s} = 200$ GeV) and the Large Hadron Collider (LHC) ($\sqrt{s} = 7$ TeV) energies.

1.1 Theoretical preliminaries

The isolated prompt photon cross-section is found more advantageous than the inclusive prompt photon cross-section [12,13]. The collider experiments always perform isolated photon measurement in order to identify the prompt photon signal from the large background of secondary decay photons. In addition, the isolation criterion makes the total photon cross-section much less sensitive to the non-perturbative fragmentation process enabling us to study the small x behaviour of gluon distribution more precisely. A photon is said to be isolated if the accompanying hadronic transverse energy ($E_{\text{T}}^{\text{had}}$) inside the isolation cone is less than some specified value ($E_{\text{T}}^{\text{iso}}$):

$$E_{\text{T}}^{\text{had}} \leq E_{\text{T}}^{\text{iso}} \text{ inside } R, \quad (1)$$

where we considered a cone of radius $R(= \sqrt{(y - y_{\gamma})^2 + (\phi - \phi_{\gamma})^2})$ in the rapidity (y) and the azimuthal angle (ϕ) space about the photon direction. It is shown in ref. [13] that the QCD factorization theorem is valid in all orders of perturbation theory with the above general isolation criterion (eq. (1)). Hence the isolated prompt photon cross-section is a perturbatively well-defined quantity like the inclusive case. In the experiment, sometimes the isolation energy is expressed in terms of a dimensionless parameter $\varepsilon = E_{\text{T}}^{\text{iso}}/p_{\text{T}}^{\gamma}$. We write the single isolated prompt photon production cross-section as [12,13]

$$\begin{aligned} E_{\gamma} \frac{d^3\sigma^{\text{iso}}}{d^3p_{\gamma}}(y_{\gamma}, p_{\gamma}, R) &= \sum_{i,j} \int dx_1 f_{i/A}(x_1, \mu_{\text{f}}^2) \\ &\times \int dx_2 f_{j/B}(x_2, \mu_{\text{f}}^2) \sum_{c=q,g} \int \frac{dz}{z^2} D_{c/\gamma}(z, \mu_{\text{F}}^2) \\ &\times \hat{\sigma}_{ij \rightarrow cX}^{\text{iso}}(p_c, x_1, x_2; z_c, R; \mu_{\text{f}}, \mu_{\text{R}}, \mu_{\text{F}}) \Theta(z - z_c), \end{aligned} \quad (2)$$

where the f_s are called the parton distribution functions (PDFs), which give the probability for the incoming partons i and j carrying momentum fractions x_1 and x_2 inside the hadrons A and B respectively. $D_{c/\gamma}(z, \mu_F^2)$ gives the parton to photon fragmentation probability defined at $z = p_\gamma/p_c$. When a photon is emitted from ‘direct’ hard interaction (i.e. $c = \gamma$), the photon fragmentation function reduces to $\delta(1 - z)$. Following the isolation criterion (1), we find that the fraction z should be $\geq 1/(1 + \varepsilon) = z_c$ [13]. Thus, for small values of ε , the fragmentation process is less contributory to the total photon cross-section compared to the direct process. This is contrary to the inclusive prompt photon production. The fragmentation function $D_{c/\gamma}(z, \mu_F^2)$ that appears in eq. (2) is the same as in case of inclusive photon production. $\hat{\sigma}^{\text{iso}}$, the isolated partonic interaction cross-section, contains all processes upto $\mathcal{O}(\alpha_s^2)$ (for $c = \gamma$) and upto $\mathcal{O}(\alpha_s^3)$ (for $c \neq \gamma$) of the reaction $i + j \rightarrow c + X$. The dependence of the isolation parameters (R, ε) is fully encoded into the isolated cross-section ($\hat{\sigma}^{\text{iso}}$). μ_f, μ_R and μ_F are the three different scales associated with the factorization, renormalization and fragmentation, respectively.

2. Results

With this theoretical introduction, now we show the results of isolated prompt photon production for $p + p$ collisions at the RHIC and LHC centres of mass energies (figure 1). Our calculation is based on the Monte Carlo program JETPHOX [14], which evaluates direct and fragmentation photon cross-section separately at NLO accuracy. We sum the two contributions to get the total physical cross-section at NLO. JETPHOX is found to explain the isolated prompt photon data at the Tevatron energy [3] and at the LHC

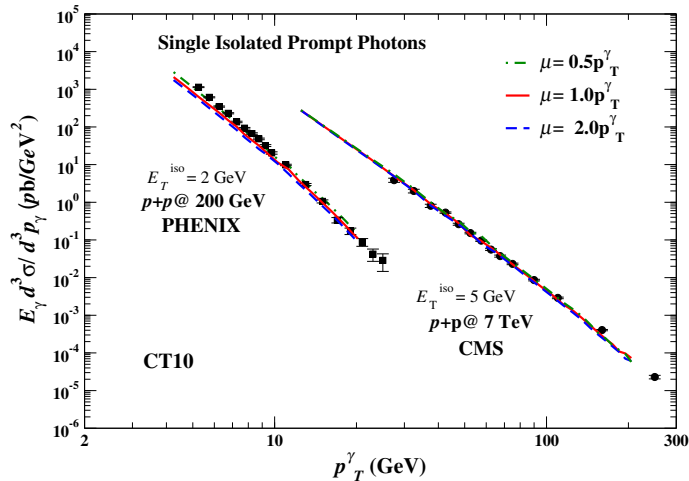


Figure 1. Scale dependence of single isolated prompt photon production in $p + p$ collisions at the RHIC (200 GeV) and LHC (7 TeV) centre of mass energies, calculated with CT10 PDF and BFG-I fragmentation function and compared with the measurements from the PHENIX and the CMS Collaborations.

energy [2,15]. This program is very useful in the sense that one can define a variety of experimental requirements (kinematic, isolation) at the partonic level. Numerous sets of PDF are made available in JETPHOX through the LHAPDF library [16]. We have considered an isolation cone of radius $R = 0.4$ and constant isolation energy cut in these studies. The parameters of calculations at the RHIC are $p_T^\gamma = 4\text{--}20$ GeV, $|y_\gamma| < 0.5$, $E_T^{\text{iso}} = 2$ GeV and at the LHC are $p_T^\gamma = 10\text{--}200$ GeV, $|y_\gamma| < 1.5$, $E_T^{\text{iso}} = 5$ GeV. We have used the BFG-I parton to photon fragmentation function by Bourhis *et al* [17], which includes correction in the fragmentation function beyond leading logarithmic approximation. The three scales μ_f, μ_R, μ_F are set equal to a common scale μ to reduce theoretical uncertainties in the calculation. The scale μ is further defined as $c p_T^\gamma$ with $c = 0.5, 1.0, 2.0$. The scale dependence of the isolated prompt photon production, calculated with CT10 PDF [18], is shown in figure 1. The results are plotted against the prompt photon measurement by the PHENIX Collaboration at midrapidity [6] and by the CMS Collaboration in the rapidity range $0.9 < \eta < 1.44$ [15]. Our results quite agree with the theoretical curve mentioned in refs [6,15]. The scale $\mu = 1.0 p_T^\gamma$ is found to be a better choice though the relative uncertainty between the scales have been found very small.

Next we have considered four more parametrizations of PDF, namely CTEQ4M [19], CTEQ6M [20], MRST2001 [21,22] and NNPDF1.0 [23]. Our motivation is to check whether the single-prompt photon yield is able to distinguish between these PDF sets. We do hope that the recent prompt photon measurements at the RHIC and LHC experiments can constrain the gluon density in the proton. The invariant prompt photon yield calculated with the five PDFs at the RHIC and the LHC energies are displayed in figure 2. We see that starting from very old parametrization like CTEQ4M to a recent parametrization like CT10 gives reasonably good description of the data within the statistical errors. A little wiggling observed at different theoretical curves for $p_T^\gamma > 12$ GeV at the RHIC and for $p_T^\gamma > 120$ GeV at the LHC can be attributed to the Monte Carlo technique of integration.

The direct and fragmentation contributions to the isolated photon cross-section ($d\sigma/dp_T^\gamma dy_\gamma$) at NLO are shown individually in figure 3. The NLO corrections to the direct contribution is due to additional real and virtual gluon emission at the LO processes $qg \rightarrow q\gamma$ and $q\bar{q} \rightarrow g\gamma$ [24]. NLO correction to the fragmentation contribution is coming from generic $\mathcal{O}(\alpha_s^3)$ subprocesses $i + j \rightarrow c + d + e$, where the parton c fragments into a photon [25,26]. All these higher-order corrections are included in JETPHOX according to the \overline{MS} renormalization and factorization schemes. It is known indeed that the total cross-section is the only physical quantity at NLO because a direct $\mathcal{O}(\alpha_s^2)$ process like $qg \rightarrow qg\gamma$ contributes similar like LO fragmentation process when the fragmentation scale μ_F is close to 1 GeV [13]. We expect that qg (or $q\bar{g}$)-initiated ‘direct’ photons could be a good probe to track down the varying gluon distribution $g(x, Q^2)$ among the PDF sets. However, as shown in figure 3, we have not found any dependence of the direct and fragmentation contributions to the PDF at the RHIC and the LHC energies. The fragmentation contribution shown in figure 3 is scaled down by a factor of 10 for better visibility. We find that the direct component has dominant contribution ($\sim 80\text{--}90\%$) to the total photon cross-section at the RHIC and the LHC energies.

We have plotted our results on logarithmic scale, which can easily consume a factor of 2–3 difference among the PDFs. To measure the deviation in the isolated prompt photon yield of different PDF sets, we introduce a parameter $\Delta_{\text{PDF}} = (\text{Modern} - \text{Old})/\text{Old}$.

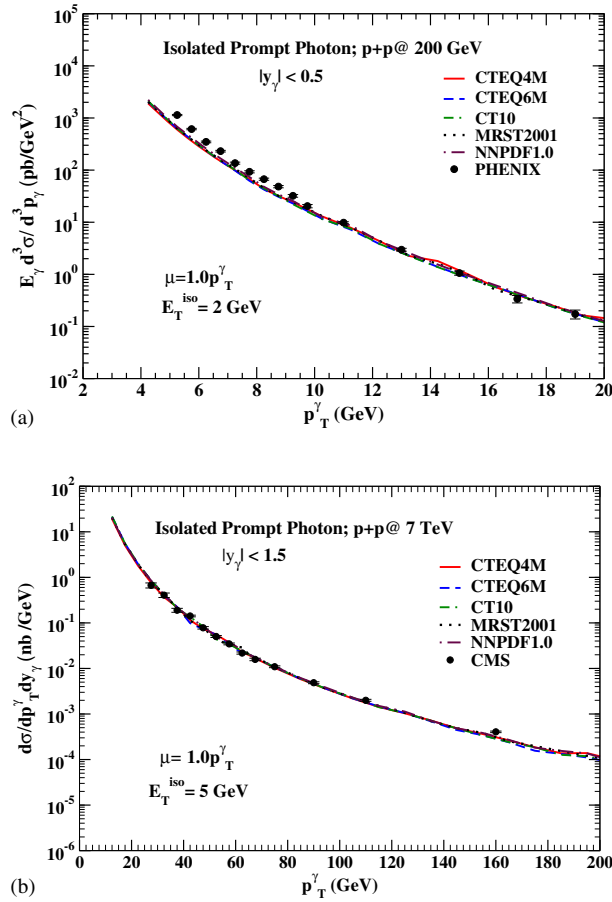


Figure 2. (a) Comparison of differential cross-section of isolated prompt photons calculated with CTEQ4M, CTEQ6M, CT10, MRST2001, NNPDF1.0 PDF, BFG-I fragmentation function and scale $\mu = 1.0 p_T^\gamma$ for $p + p$ collisions at the RHIC energy. (b) The same for $p + p$ collisions at the LHC energy.

The ‘Old’ refers to the isolated prompt photon cross-section calculated with CTEQ4M. The ‘Modern’ refers to the same calculated with CTEQ6M, CT10, MRST2001 and NNPDF1.0. Thus, the CTEQ4M is chosen as the central value and Δ_{PDF} measures the deviation as we go towards newer structure functions. The dependence of Δ_{PDF} with p_T^γ at the RHIC and the LHC energies are displayed in figure 4. Apart from the numerical fluctuations, we find all the PDFs show a monotonic variation with p_T^γ . Δ_{PDF} of CTEQ6M first decreases for $p_T^\gamma \leq 10 \text{ GeV}$ at the RHIC and $p_T^\gamma \leq 40 \text{ GeV}$ at the LHC, then increases with p_T^γ . The amount of deviation is seen least for MRST2001 and most for NNPDF1.0. It is found that the uncertainty in the isolated prompt photon cross-section associated with the choice of PDFs is within 20% at the RHIC and LHC energies for all p_T^γ . Similar work at the Tevatron energy can be found in ref. [27] where the comparison is made with three PDFs and the prediction is made for $p + p$ collisions at the top

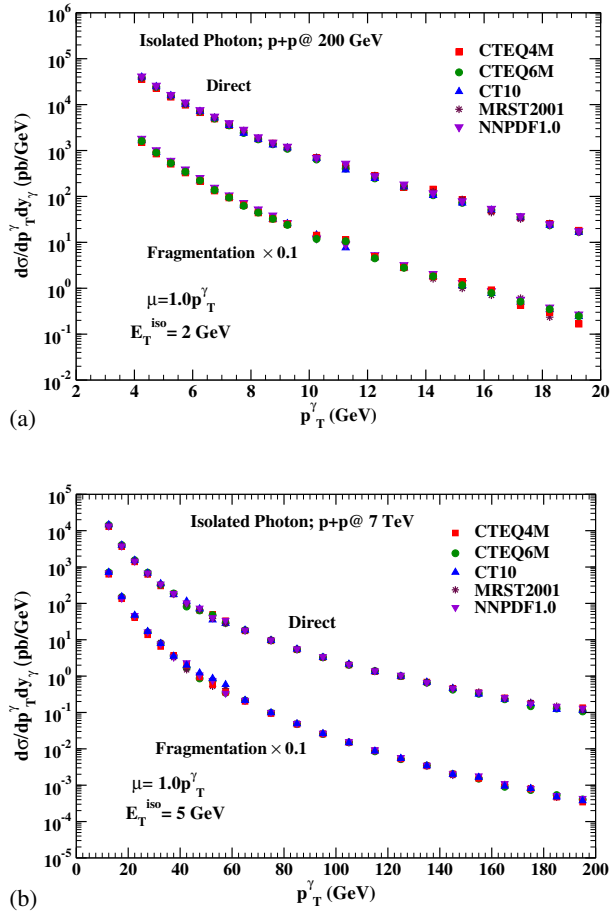


Figure 3. The ‘direct’ and ‘fragmentation’ contributions to total isolated prompt photon production in $p + p$ collisions are displayed for the five different PDFs at the RHIC (a) and the LHC energies (b). The ‘fragmentation’ component is scaled by 0.1.

LHC energy ($\sqrt{s} = 14$ TeV). A recent quantitative study using a particular PDF set and its replicas at different collider energies have drawn a similar conclusion [28].

Finally, we have checked the variation of gluon distribution $g(x, Q^2)$ among the five different parametrizations of PDF in the kinematic regime, $10^{-3} \leq x \leq 10^{-1}$, probed by the present RHIC and LHC photon data. In figure 5, we have plotted the momentum density of gluons $xg(x, Q^2)$ vs. the momentum fraction x for a typical value of $Q^2 = 80$ GeV². This shows that the gluon distribution is varying indeed among the five PDFs considered in this study. Thus, we believe that the sensitivity of single-prompt photon production to the parton distributions is taken away due to the integration over the initial parton momenta x_1 and x_2 in eq. (2).

However, the double-prompt photon production cross-section in hadronic collisions is directly proportional to the incoming parton momentum density (or the PDF) [29,30].

Extent of sensitivity of single photon

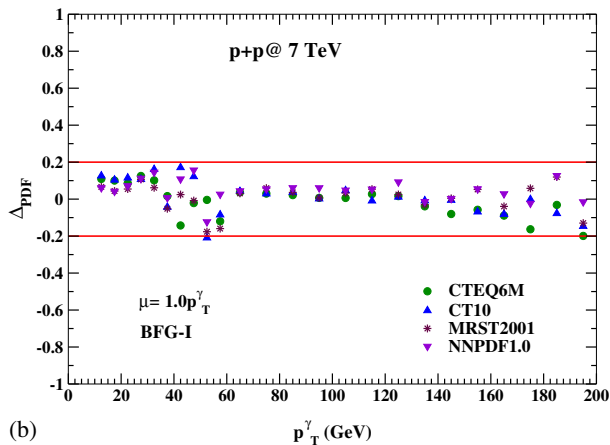
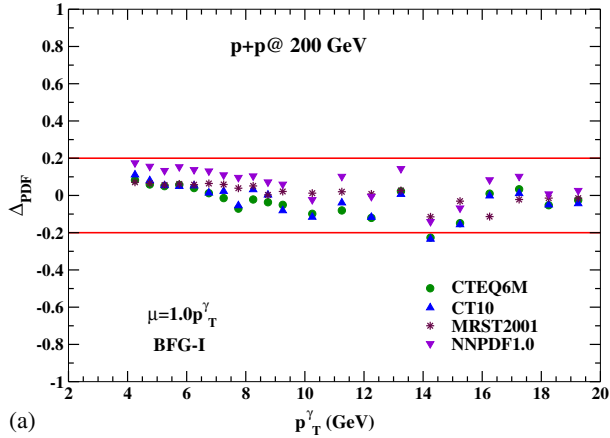


Figure 4. The PDF uncertainty in the isolated prompt photon production in $p + p$ collisions related to the choice of PDF is plotted with the transverse momentum of photon (p_T^γ) at the RHIC (a) and LHC (b) energies.

The double-prompt photons produced through quark–antiquark annihilation $q\bar{q} \rightarrow \gamma\gamma$ or gluon–gluon fusion $gg \rightarrow \gamma\gamma$ completely specify parton momentum distribution. The single bremsstrahlung contribution like $qg \rightarrow q\gamma\gamma$ to the double photon production is also sensitive to the PDF. Hence, we hope the double-prompt photon measurement at the LHC energy could better probe the gluon distribution $g(x, Q^2)$ in the proton in comparison with the single-prompt photon measurement.

3. Summary and outlook

We have analysed the data of single-prompt photon production in $p + p$ collisions at the centre of mass energies 200 GeV (RHIC) and 7 TeV (LHC) with five different

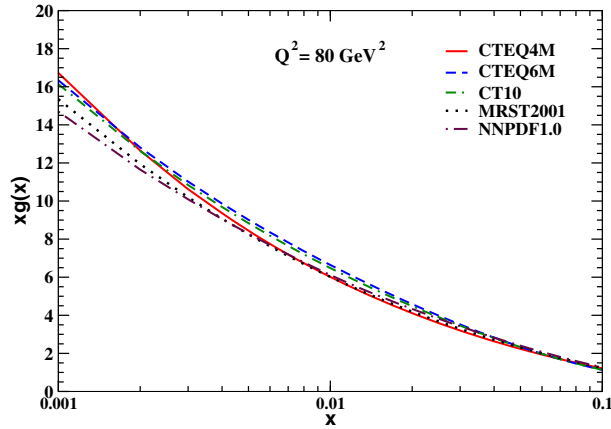


Figure 5. The gluon momentum density $xg(x, Q^2)$ vs. the momentum fraction x for the five PDFs considered in the present study for a typical value of momentum transfer square $Q^2 = 80 \text{ GeV}^2$.

parametrizations of PDF. Our calculation relies on the available program `JETPHOX`, which calculates isolated prompt photon production at the NLO accuracy. We have shown that the single isolated prompt photon momentum spectra is almost insensitive to the choice of PDF, which is due to the integration over the initial-state parton momenta. The present analysis suggests that the recent prompt photon measurements at the RHIC and LHC can constrain the gluon distribution inside proton not more than 20% of certainty. We expect that the differential production cross-section of double-prompt photons can determine the gluon distribution more precisely and shall be checked in future studies.

Acknowledgements

SD is thankful to Dinesh Srivastava and Rupa Chatterjee for many stimulating discussions and comments on the manuscript. The author sincerely acknowledges the useful correspondences with Jean-Philippe Guillet regarding `JETPHOX`. The author is financially supported by Department of Atomic Energy, India, during the course of this work.

References

- [1] J F Owens, *Rev. Mod. Phys.* **59**, 465 (1987)
- [2] ATLAS Collaboration: G Aad *et al*, *Phys. Rev. D* **83**, 052005 (2011)
- [3] CDF Collaboration: T Aaltonen *et al*, *Phys. Rev. D* **80**, 111106 (2009)
- [4] D0 Collaboration: V M Abazov *et al*, *Phys. Lett. B* **639**, 151 (2006); Erratum, *ibid. B* **658**, 285 (2008)
- [5] PHENIX Collaboration: S S Adler *et al*, *Phys. Rev. Lett.* **98**, 012002 (2007)
- [6] PHENIX Collaboration: A Adare *et al*, *Phys. Rev. D* **86**, 072008 (2012)
- [7] P Aurenche, R Baier, M Fontannaz, J F Owens and M Werlen, *Phys. Rev. D* **39**, 3275 (1989)
- [8] H Baer, J Ohnemus and J F Owens, *Phys. Rev. D* **42**, 61 (1990)

- [9] W Vogelsang and A Vogt, *Nucl. Phys. B* **453**, 334 (1995)
- [10] F Arleo, *J. High Energy Phys.* **0609**, 015 (2006)
- [11] W Vogelsang and M R Whalley, *J. Phys. G* **23**, A1 (1997)
- [12] E L Berger and J Qiu, *Phys. Rev. D* **44**, 2002 (1991)
- [13] S Catani, M Fontannaz, J P Guillet and E Pilon, *J. High Energy Phys.* **0205**, 028 (2002)
- [14] P Aurenche, J P Guillet, E Pilon, M Werlen and M Fontannaz, *Phys. Rev. D* **73**, 094007 (2006); <http://lapth.cnrs.fr/PHOXFAMILY/jetphox.html>
- [15] CMS Collaboration: S Chatrchyan *et al*, *Phys. Rev. D* **84**, 052011 (2011)
- [16] <http://www.hepforge.org/downloads/lhapdf>
- [17] L Bourhis, M Fontannaz and J P Guillet, *Eur. Phys. J. C* **2**, 529 (1998)
- [18] H L Lai *et al*, *Phys. Rev. D* **82**, 074024 (2010)
- [19] H L Lai *et al*, *Phys. Rev. D* **55**, 1280 (1997)
- [20] J Pumplin *et al*, *J. High Energy Phys.* **0207**, 012 (2002)
- [21] A D Martin *et al*, *Eur. Phys. J. C* **23**, 73 (2002)
- [22] A D Martin *et al*, *Eur. Phys. J. C* **28**, 455 (2003)
- [23] NNPDF Collaboration: R D Ball *et al*, *Nucl. Phys. B* **809**, 1 (2009); Erratum, *ibid. B* **816**, 293 (2009)
- [24] P Aurenche, R Baier, M Fontannaz and D Schiff, *Nucl. Phys. B* **297**, 661 (1988)
- [25] F Aversa, P Chiappetta, M Greco and J P Guillet, *Phys. Lett. B* **210**, 225 (1988)
- [26] P Aurenche, P Chiappetta, M Fontannaz, J P Guillet and E Pilon, *Nucl. Phys. B* **399**, 34 (1993)
- [27] R Ichou and D d'Enterria, *Phys. Rev. D* **82**, 014015 (2010)
- [28] D d'Enterria and J Rojo, *Nucl. Phys. B* **860**, 311 (2012)
- [29] E L Berger, E Braaten and R D Field, *Nucl. Phys. B* **239**, 52 (1984)
- [30] R D Field, *Applications of perturbative QCD* (Addison-Wesley Publishing Company)